Databasing Molecular Imaging

Finn Årup Nielsen

Neurobiology Research Unit, Rigshospitalet
and
Informatics and Mathematical Modelling
Technical University of Denmark

September 16, 2004

Databasing Molecular Imaging

Databasing $\underset{\text{Here!}}{=}$ Representation, retrieval and (meta-)analysis of results from the literature

Molecular neuroimaging =

Positron emission tomography or autoradiography +

neurotransmitter receptors, ...

Brede database

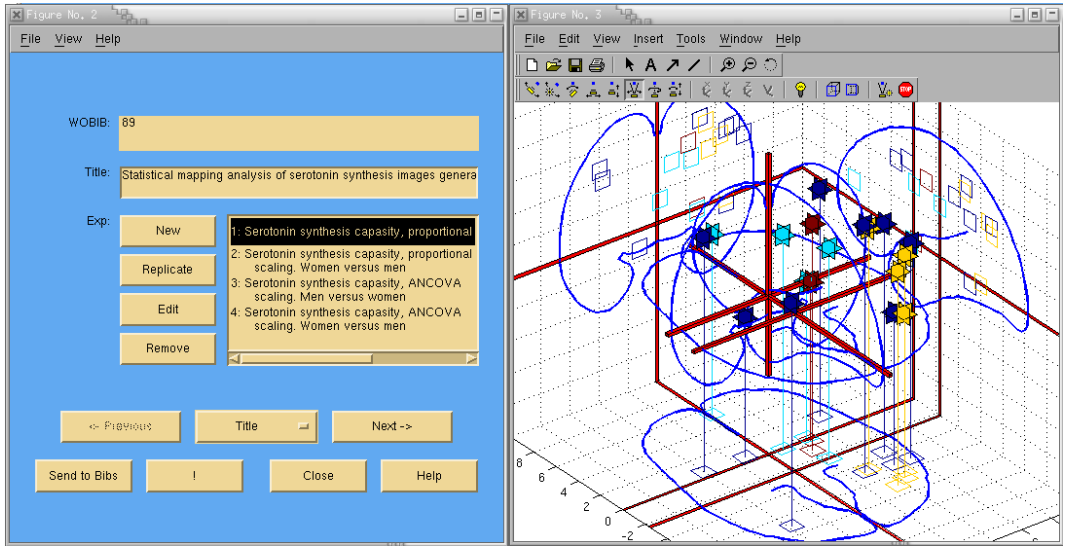

Figure 1: Screenshot of main window of Matlab program for data entry of (Okazawa et al., 2000).

Brede neuroinformatics database (Nielsen, 2003).

Main components: "locations", i.e., stereotaxic coordinates reported in standardized "Talairach" space (Talairach and Tournoux, 1988).

Linked to PubMed, MeSH, fMRIDC, SenseLab, NeuroNames.

"Poor man's XML" (pXML): Database kept in a simplified version of XML, distributable on the internet.

WOEXP: 390 - Increased benzodiazepine receptor binding in panic disorder

Bib -> Asymmetry | Author | ICA | NMF | Novelty | Statistics | SVD | Title | WOBIB]
Exp -> Alphabetic | Asymmetry | ICA | NMF | Novelty | SVD | WOEXP | WOEXT]
Ext -> Alphabetic index | Map | Roots] [Brede] Loc -> Statistics]

[WOEXP_390] **Increased benzodiazepine receptor binding in panic disorder**. *Increased benzodiazepine receptor binding in panic disorder in panic disorder patients versus normal control subjects.*
WOEXP: 390.

J. D. Bremner; R. B. Innis; T. White; M. Fujita; D. Silbersweig; A. W. Goddard; L. Staib; E. Stern; A. Cappiello; S. Woods; R. Baldwin; D. S. Charney. *SPECT [I-123]iomazenil measurement of the benzodiazepine receptor in panic disorder.*. *Biol Psychiatry* **47**(2):96-106, 2000. PMID: 10664825. WOBIB: 126.

Disease - Panic disorder
WOEXT: 234.
WOEXT: 380.

Modality:	SPECT/MRI
Measured variable:	Distribution volume
Tracer:	I-123 Iomazenil
Scanner:	Digital Scintigraphics CERASPECT
Number of subjects:	29

Asymmetry: -0.27344 (left: -1, right: +1)

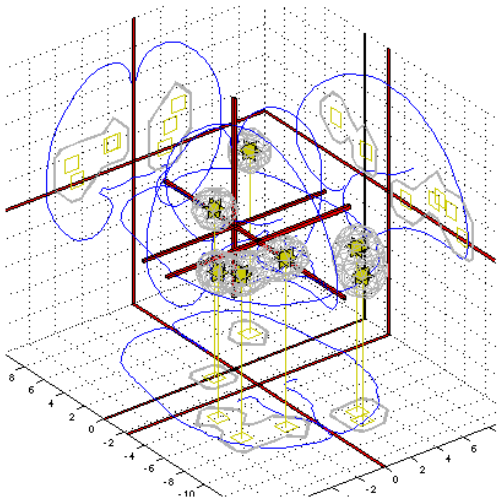

[PNG | VRML (87Kb)]

x	y	z	Lobar anatomy	Functional area	WOROI	Value
-16	-1	18	Right caudate			
-18	-75	18	Cuneus (occipital cortex)			
34	29	28	Right middle frontal gyrus			

Brede data model inspired by BrainMap database (Fox and Lancaster, 1994): Paper (bibliographic information), experiment (summary image, tracer, scanner, paradigm, stimulus/response), location (stereotactic coordinates).

Data entry with a Matlab program for the information in "experiments" and "locations".

“External components”

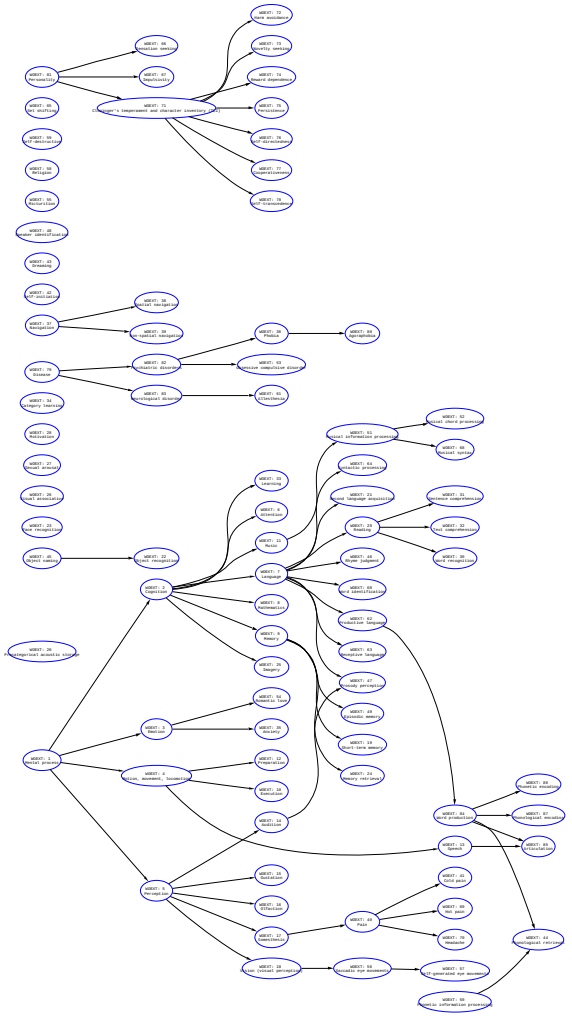

External components, e.g., cognitive components, “Cold pain”, “Alzheimer’s disease”, “BZ site GABA-A receptor”

External components represented in a directed acyclic graph (causal network).

Corresponding to MeSH (NLM Medical Subject headings), linking to MeSH and Wikipedia, bioinformatics services where equivalent items exist.

Presently 438 components.

WOEXT: 23. **Face recognition**.
Processing of face images.

Parents	Siblings	Children
Visual object recognition		

Experiments:

1. **Face visual object**. *Visual objects: Faces versus building*. WOEXP: 11.
   I Levy; U Hasson; G Avidan; T Hendler; R Malach. *Center–periphery organization of human object areas.*. *Nat Neurosci* **4**(5):533–9, 2001.
   PMID: 11319563. WOBIB: 5.
2. **Photographs of faces versus houses and chairs**. *Conjunction between passive viewing and delayed match–to sample of gray–scale photographs versus scrambled pictures and faces versus houses and chairs, with matching choice indicated by pressing a button with the right of left thumb*. WOEXP: 91.
   A. Ishai; L. G. Ungerleider; A. Martin; J. V. Haxby. *The representation of objects in the human occipital and temporal cortex.*. *J Cogn Neurosci* **12 Suppl 2**:35–51, 2000.
   PMID: 11506646. FMRIDCID: 2–2000–1113D.
   WOBIB: 28.
3. **Front–face**. *Line drawings of front face versus line drawings of tumblers*. WOEXP: 123.
   U. Hasson; T. Hendler; D. Ben Bashat; R. Malach. *Vase or face? A neural correlate of shape–selective grouping processes in the human brain.*. *J Cogn Neurosci* **13**(6):744–53, 2001.
   PMID: 11564319. FMRIDCID: 2–2001–111P8.
   WOBIB: 36.

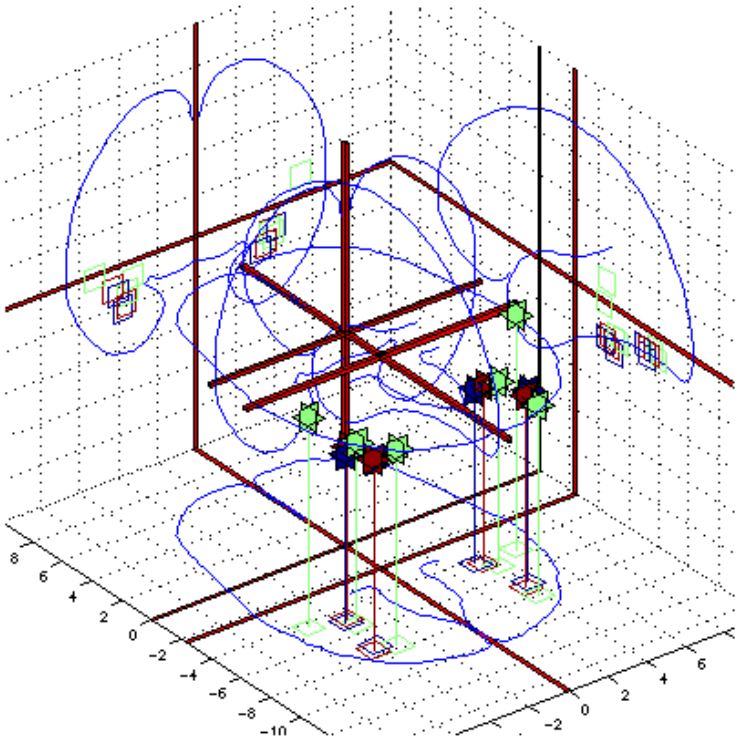

Web-pages generated for each component

Corner Cube visualization (Rehm et al., 1998) with experiments that relates to the specific external component.

Clickable graphs generated with *dot* (Koutsofios and North, 1996).

Modeling locations and volumes

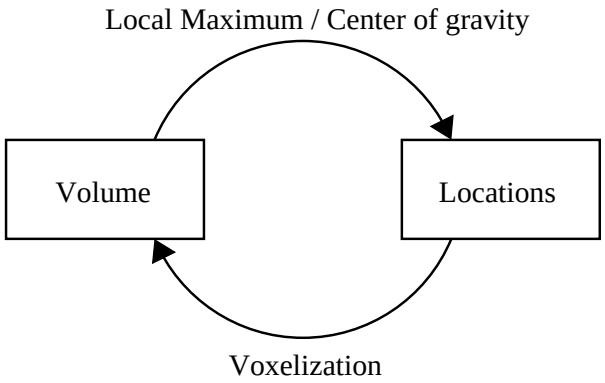

Regard the "locations" as being generated from a distribution $p(\mathbf{x})$, where $\mathbf{x}$ is in 3D Talairach space (Fox et al., 1997).

Kernel methods (N kernels centered on each object: $\boldsymbol{\mu}_n$) with homogeneous Gaussian kernel in 3D Talairach space $\mathbf{x}$

$$\widehat{p}(\mathbf{x}) = \frac{(2\pi\sigma^2)^{-3/2}}{N} \sum_n^N e^{-\frac{1}{2\sigma^2}(\mathbf{x}-\boldsymbol{\mu}_n)^2}$$

σ^2 fixed or optimized with leave-one-out cross-validation (Nielsen and Hansen, 2002).

Condition on, e.g., anatomical label, behavioral domain c: $p(\mathbf{x}|c)$

Finding related volumes

[WOEXP 89] **Passively viewed scenes.** *Passive viewing of outdoor scenes, furnished rooms, landscapes and landmarks.* WOEXP: 89.

R. Epstein; N. Kanwisher. *A cortical representation of the local visual environment.* *Nature* **392**(6676):598–601, 1998. PMID: 9560155. DOI: 10.1038/33402. WOBIB: 27.

Perception,Vision – Places

Modality: fMRI

Asymmetry: 0.00000 (left: −1, right: +1)

VRML97 file (61 Kb)

x	y	z	Lobar anatomy	Functional area
18	−39	−6		Parahippocampal place area
−34	−42	−6		Parahippocampal place area

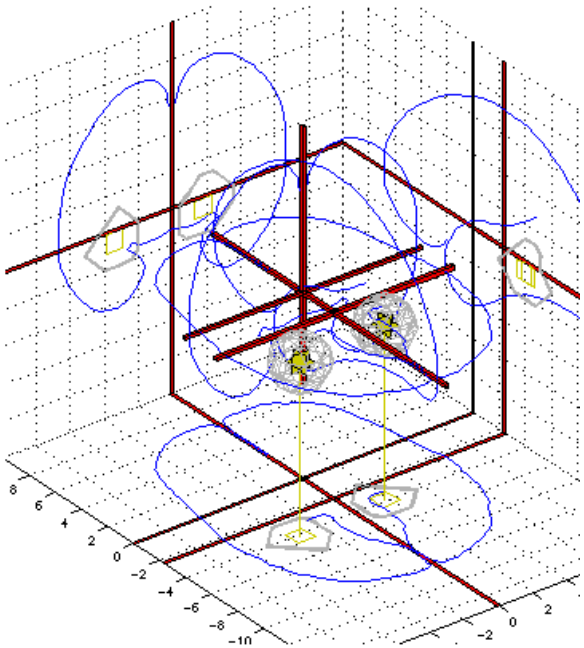

Related – positive correlated volumes

+2: 0.80010 (12) **Buildings visual objects.** *Visual object stimuli: Building versus faces.* WOEXP: 12.
I Levy; U Hasson; G Avidan; T Hendler; R Malach. *Center–periphery organization of human object areas.* *Nat Neurosci* **4**(5):533–9, 2001. PMID: 11319563. DOI: 10.1038/87490. WOBIB: 5.

+3: 0.49922 (42) **Attention to musical instruments versus attention to consonant–vowels.** *Attend to sound and press a button when the target stimulus appeared.* WOEXP: 42.
K. Hugdahl; I. Law; S. Kyllingsbaek; K. Bronnick; A. Gade; O. B. Paulson. *Effects of attention on dichotic listening: an 150–PET study.* *Hum Brain Mapp* **10**(2):87–97, 2000. PMID: 10864233. WOBIB: 14.

+4: 0.45377 (97) **Visual object decision.** *Visual object decision with novel and chimeric, natural and artefact line drawings versus pattern discrimination.* WOEXP: 96.
C. Gerlach; I. Law; A. Gade; O. B. Paulson. *Perceptual differentiation and category effects in normal object recognition: a PET study.* *Brain* **122 (Pt 11)**:2159–70, 1999. PMID: 10545400. WOBIB: 29.

Each experiment a volume: $p(\mathbf{x}|\text{experiment} = \text{WOBIB } 89)$ sampled on a fixed 8mm grid.

Sorted list of similar volumes (Nielsen and Hansen, 2004)

Figure shows result page with automatically generated corner cube visualization of an experiment (Epstein and Kanwisher, 1998).

However . . .

Most molecular imaging studies are not based on stereotaxic coordinates.

Most molecular imaging studies relies on analysis of values from brain regions and report descriptive statistics for these values.

Regions differ between studies: E.g., some include values for "temporal cortex" others do not.

Measured and reported values differ between studies and they are not comparable: Tracers and receptors; transport rates (e.g., K_1), distribution volume, binding potentials; different methods to compute the values.

Brain anatomy description

WOROI: 5 - Posterior cingulate gyrus

Bib -> Asymmetry | Author | ICA | NMF | Novelty | Statistics | SVD | Title | WOBIB]

Roi -> Alphabetic | Hammers | Tzourio-Mazoyer]

[Brede]

WOROI: 5 - Posterior cingulate gyrus

Abbreviation: **PCgG**

Variation: *posterior cingulate*
Variation: *posterior cingulate area*
Variation: *posterior gyrus cinguli*
BrainInfo: 144

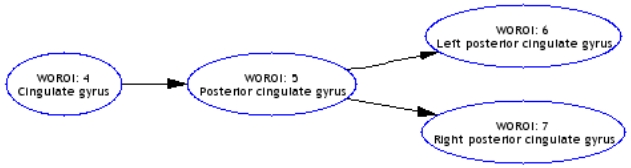

Parents	Siblings	Children
Cingulate gyrus		Left posterior cingulate gyrus Right posterior cingulate gyrus

Talairach coordinates

x	y	z	Lobar anatomy	WOBIB	WOEXP
6	-29	38	Right posterior cingulate gyrus and precuneus	21	66
9	-53	14	Right posterior cingulate gyrus	32	109
4	-53	14	Right posterior cingulate gyrus	32	110
2	-40	40	Posterior cingulate gyrus	35	117
52	-30	20	Right postcentral gyrus/posterior cingulate gyrus	35	119
-4	-36	24	Left posterior cingulate gyrus	41	135
-4	-35	29	Left posterior cingulate gyrus	41	137
-4	-35	40	Left posterior cingulate gyrus	41	138
0	-26	29	Posterior cingulate gyrus	41	140
-2	-48	20	Left posterior cingulate gyrus	49	164
-9	-33	46	Posterior cingulate gyrus	57	183
0	-17	28	Right posterior cingulate gyrus	60	186
3	-53	15	Right posterior cingulate gyrus	71	223

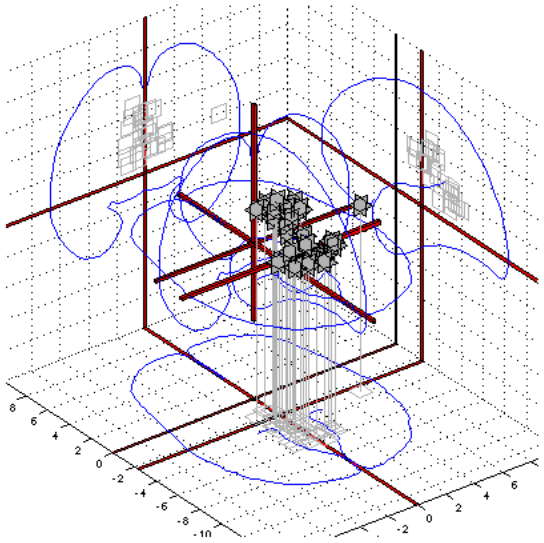

To handle the difference between brain region schemes a taxonomy (simple ontology) of brain regions is constructed.

Records which brain areas are a part of other brain areas.

Links to NIH MeSH, BrainInfo (NeuroNames), segmented volumes, Wikipedia.

Clustering

	ACC	Cx	TL	FL	PL	OL	Cb	Th	Amg	Pu	Cd	Pons	Brain stem	WM
Altanserin	0.42	—	—	—	0.73	1.09	-1.79	-0.90	—	—	-1.17	-1.44	—	—
Age depend	-0.84	—	—	—	0.62	—	—	—	—	—	—	—	—	—
Radiactivi	—	—	-0.81	-0.93	-0.34	0.01	-1.04	1.77	—	—	—	—	—	—
Distributi	—	—	-0.43	-0.87	0.76	-0.72	-1.32	1.50	—	—	—	—	—	—
Altanserin	—	—	—	—	—	—	-1.52	-0.69	-0.83	-0.91	-0.78	—	—	—
Mu-opioid	-0.04	—	-0.28	—	-0.60	-1.71	-1.00	1.31	0.67	0.99	1.47	-0.44	—	—
Mu-opioid	-0.09	—	-0.31	—	-0.67	-1.83	-0.67	1.36	0.71	0.71	1.58	-0.38	—	—
Time to pe	—	0.77	1.13	0.42	0.42	0.77	-0.63	-1.29	—	0.77	—	—	-1.78	-0.59
Distributi	—	0.05	0.03	0.00	0.23	0.09	0.83	0.97	—	0.86	—	—	-0.57	-2.50
Distributi	—	0.29	0.37	0.24	0.39	0.15	0.62	0.60	—	0.97	—	—	-1.42	-2.20
Fluroethyl	—	—	0.29	0.39	—	1.34	0.09	-0.44	—	—	—	-1.66	—	—
Fluroethyl	—	—	0.29	0.41	—	1.33	0.10	-0.46	—	—	—	-1.66	—	—
Flumazenil	—	—	0.72	0.56	—	1.16	-0.40	-0.48	—	—	—	-1.56	—	—
Flumazenil	—	—	0.71	0.56	—	1.16	-0.39	-0.48	—	—	—	-1.56	—	—
Flumazenil	—	-0.86	—	-0.86	—	0.39	-0.55	1.33	—	1.33	0.39	-1.17	—	—

Data matrix $\mathbf{X}$(experiments $\times$ regions).

Clustering of studentized values with the K-means algorithm in a version capable of handling missing values: $\mathbf{X} = \mathbf{AC} + \mathbf{U}$ or $\mathbf{X} = \mathbf{CA} + \mathbf{U}$

Altanserin binding to 5-HT2A receptors. *Altanserin binding to 5-HT2A receptors as partial volume corrected distribution volume (DV'3) with cerebellum as reference region.*	1	0	0	0	0
Age dependence on altanserin binding to 5-HT2A receptors. *Age dependence on altanserin binding to 5-HT2A receptors as partial volume corrected distribution volume with cerebellum as reference region.*	0	0	0	0	1
Radiactivity distribution of vinpocetine. *Ratio of radiactivity distribution values of vincepoteine in the period from 9 to 57 minutes after administration with cerebellum as the reference region.*	0	0	1	0	0
Distribution volume ratio of vinpocetine. *Distribution volume ratio of vinpocetine with cerebellum as the reference region.*	0	0	1	0	0
Altanserin binding to 5-HT(2A) receptor. *Altansering binding to 5-HT(2A) receptor.*	1	0	0	0	0
Mu-opioid receptor binding in men. *Mu-opioid receptor binding potential in men.*	0	0	1	0	0
Mu-opioid receptor binding in women. *Mu-opioid receptor binding potential in women.*	0	0	1	0	0
Time to peak for MTHA. *Kinetics time to peak for MTHA (methyl-tetrahydro-aminoacridine) after injection.*	0	0	0	1	0
Distribution of MTHA at peak. *Distribution of MTHA (methyl-tetrahydro-aminoacridine) at peak of concentration.*	0	1	0	0	0
Distribution of MTHA between 50-70 minutes. *Distribution of MTHA (methyl-tetrahydro-aminoacridine) between 50-70 after injection.*	0	1	0	0	0
Fluroethylflumazenil distribution volume for the benzodiazepine receptor. *Fluroethylflumazenil distribution volume for the benzodiazepine receptor.*	0	0	0	0	1
Fluroethylflumazenil binding to the benzodiazepine receptor. *Fluroethylflumazenil binding potential for the benzodiazepine receptor with pons as the reference region.*	0	0	0	0	1
Flumazenil distribution volume for the benzodiazepine receptor. *Flumazenil distribution volume for the benzodiazepine receptor.*	0	0	0	0	1
Flumazenil binding to the benzodiazepine receptor. *Flumazenil binding potential for the benzodiazepine receptor with pons as the reference region.*	0	0	0	0	1
Flumazenil K1 rate constant for the benzodiazepine receptor, first experiment. *Flumazenil K1 rate konstant for the benzodiazepine receptor.*	0	0	1	0	0
Flumazenil distribution volume for the benzodiazepine receptor, first experiment. *Flumazenil distribution volume for the benzodiazepine receptor.*	0	0	0	0	1

Summary

Modeling 3D Talairach coordinates with kernel density estimators.

Modeling of regional data.

Brede neuroinformatics toolbox: Primarily written in Matlab. Includes the Brede database in XML. http://hendrix.imm.dtu.dk/software/brede/.

Results available on the Internet from hendrix.imm.dtu.dk more specifically http://hendrix.imm.dtu.dk/services/jerne/.

Altanserin cluster

1.000*. **Altanserin binding to 5-HT2A receptors**. *Altanserin binding to 5-HT2A receptors as partial volume corrected distribution volume (DV'3) with cerebellum as reference region.*	**0.898-**. WOROI: 26 - Occipital lobe
1.000*. **Altanserin binding to 5-HT(2A) receptor**. *Altanserin binding to 5-HT(2A) receptor.*	**0.727***. WOROI: 21 - Parietal lobe
1.000*. **Altanserin binding to the 5-HT2A receptor**. *Altanserin binding to the 5-HT2A receptor with a 4-compartmental analysis and cerebellum as the reference region.*	**0.517***. WOROI: 8 - Anterior cingulate gyrus
	0.000-. WOROI: 14 - Cerebral Cortex
	0.000-. WOROI: 15 - Temporal lobe
	0.000-. WOROI: 18 - Frontal lobe
	0.000-. WOROI: 80 - Brain stem
	0.000-. WOROI: 219 - White matter
	-0.792-. WOROI: 34 - Thalamus
	-0.822-. WOROI: 40 - Hippocampus

Three independent altanserin studies cluster (Adams, 2003; Forutan et al., 2002; Sheline et al., 2002)

Occipital and parietal lobe the area of highest binding.

Altanserin binding to 5-HT2A receptors. *Altanserin binding to 5-HT2A receptors as partial volume corrected distribution volume (DV'3) with cerebellum as reference region.*

Karen H. Adams; Lars H. Pinborg; Claus Svarer; Steen G. Hasselbalch; Soren Holm; Steven Haugbol; Karine Madsen; Vibe Frokjaer; Lars Martiny; Olaf B. Paulson; Gitte M. Knudsen. *A database of [(18)F]-altanserin binding to 5-HT(2A) receptors in normal volunteers: normative data and relationship to physiological and demographic variables.*. *Neuroimage* **21**(3):1105-13, 2004.
PMID: 15006678. DOI: 10.1016/j.neuroimage.2003.10.046.

WOEXT: 298.

Modality:	PET/MRI
Measured variable:	Distribution volume
Tracer:	F-18 Altanserin
Scanner:	GE Medical Systems, Advance
Number of subjects:	52

Related - positive correlated volumes

+1: 1.00000 **Altanserin binding to 5-HT2A receptors**. *Altanserin binding to 5-HT2A receptors as partial volume corrected distribution volume (DV'3) with cerebellum as reference region.*
Karen H. Adams; Lars H. Pinborg; Claus Svarer; Steen G. Hasselbalch; Soren Holm; Steven Haugbol; Karine Madsen; Vibe Frokjaer; Lars Martiny; Olaf B. Paulson; Gitte M. Knudsen. *A database of [(18)F]-altanserin binding to 5-HT(2A) receptors in normal volunteers: normative data and relationship to physiological and demographic variables.*. *Neuroimage* **21**(3):1105-13, 2004.
PMID: 15006678. DOI: 10.1016/j.neuroimage.2003.10.046.

+2: 0.98925 **Altanserin binding to 5-HT(2A) receptor**. *Altanserin binding to 5-HT(2A) receptor.*
F. Forutan; S. Estalji; M. Beu; S. Nikolaus; K. Hamacher; H. H. Coenen; H. Vosberg; H. W. Muller-Gartner; R. Larisch. *Distribution of 5HT2A receptors in the human brain: comparison of data in vivo and post mortem.*. *Nuklearmedizin* **41**(4):197-201, 2002.
PMID: 12224404.

+3: 0.98809 **Altanserin binding to the 5-HT2A receptor**. *Altanserin binding to the 5-HT2A receptor with a 4-compartmental analysis and cerebellum as the reference region.*
Yvette I. Sheline; Mark A. Mintun; Stephen M. Moerlein; Abraham Z. Snyder. *Greater loss of 5-HT(2A) receptors in midlife than in late life.*. *American Journal of Psychiatry* **159**(3):430-435, 2002. PMID: 11870007. FMRIDCID: .

References

Adams, K. H. (2003). *The in vivo brain distribution of serotonin 5-HT$_{2A}$ receptors in healthy subjects and in patients with obsessive-compulsive disorder: a positron emission study with [^{18}F]-altanserin*. PhD thesis, Neurobiology Research Unit, Rigshospitalet, University Hospital of Copenhagen, Denmark.

Epstein, R. and Kanwisher, N. (1998). A cortical representation of the local visual environment. *Nature*, 392(6676):598–601. PMID: 9560155. DOI: 10.1038/33402. ISSN 0028-0836.

Forutan, F., Estalji, S., Beu, M., Nikolaus, S., Hamacher, K., Coenen, H. H., Vosberg, H., Müller-Gärtner, H.-W., and Larisch, R. (2002). Distribution of 5HT$_{2A}$ receptors in the human brain: comparison of data in vivo and post mortem. *Nuklearmedizin*, pages 197–201. http://www.schattauer.de/zs/nukl/2002/4/pdf/02040197.pdf.

Fox, P. T. and Lancaster, J. L. (1994). Neuroscience on the net. *Science*, 266(5187):994–996. PMID: 7973682.

Fox, P. T., Lancaster, J. L., Parsons, L. M., Xiong, J.-H., and Zamarripa, F. (1997). Functional volumes modeling: Theory and preliminary assessment. *Human Brain Mapping*, 5(4):306–311. http://www3.interscience.wiley.com/cgi-bin/abstract/56435/START.

Koutsofios, E. and North, S. C. (1996). *Drawing graphs with* dot. AT&T Bell Laboratories, Murray Hill, New Jersey.

Nielsen, F. Å. (2003). The Brede database: a small database for functional neuroimaging. *NeuroImage*, 19(2). http://208.164.121.55/hbm2003/abstract/abstract906.htm. Presented at the 9th International Conference on Functional Mapping of the Human Brain, June 19–22, 2003, New York, NY. Available on CD-Rom.

Nielsen, F. Å. and Hansen, L. K. (2002). Modeling of activation data in the BrainMap^{TM} database: Detection of outliers. *Human Brain Mapping*, 15(3):146–156. DOI: 10.1002/hbm.10012. http://www3.interscience.wiley.com/cgi-bin/abstract/89013001/. CiteSeer: http://citeseer.nj.nec.com/nielsen02modeling.html.

Nielsen, F. Å. and Hansen, L. K. (2004). Finding related functional neuroimaging volumes. *Artificial Intelligence in Medicine*, 30(2):141–151. PMID: 14992762. http://www.imm.dtu.dk/~fn/Nielsen2002Finding/.

Okazawa, H., Leyton, M., Benkelfat, C., Mzengeza, S., and Diksic, M. (2000). Statistical mapping analysis of serotonin synthesis images generated in healthy volunteers using positron-emission tomography and alpha-[11C]methyl-L-tryptophan. *Journal of Psychiatry & Neuroscience*, 25(4):359–370. PMID: 11022401. WOBIB: 89. ISSN 1180-4882.

Rehm, K., Lakshminarayan, K., Frutiger, S. A., Schaper, K. A., Sumners, D. L., Strother, S. C., Anderson, J. R., and Rottenberg, D. A. (1998). A symbolic environment for visualizing activated foci in functional neuroimaging datasets. *Medical Image Analysis*, 2(3):215–226. PMID: 9873900. http://www.sciencedirect.com/science/article/B6W6Y-45PJY0D-7/1/48196224354fdd62ea8c5a0d85379b07.

Sheline, Y. I., Mintun, M. A., Moerlein, S. M., and Snyder, A. Z. (2002). Greater loss of 5-HT(2A) receptors in midlife than in late life. *American Journal of Psychiatry*, 159(3):430–435. PMID: 11870007. ISSN 0002-953X.

Talairach, J. and Tournoux, P. (1988). *Co-planar Stereotaxic Atlas of the Human Brain*. Thieme Medical Publisher Inc, New York. ISBN 0865772932.